Preprints of the 21st IFAC World Congress (Virtual)
Berlin, Germany, July 12-17, 2020

On Strict Dissipativity of Systems Modeled by Convex Difference Inclusions: Theory and Application to Hybrid Electric Vehicles

Gabriele Pozzato *, **Matthias Müller** **, **Simone Formentin** *, **Sergio M. Savaresi** *

* *Dipartimento di Elettronica, Informazione e Bioingegneria, Politecnico di Milano, Piazza L. Da Vinci 32, 20133 Milano, Italy e-mail: {gabriele.pozzato,simone.formentin,sergio.savaresi}@polimi.it*

** *Institute of Automatic Control, Leibniz University Hannover, Germany e-mail: mueller@irt.uni-hannover.de*

Abstract: In this paper, strict dissipativity conditions are derived for the optimal steady-state operation of dynamical systems described by convex difference inclusions. This result guarantees convergence to a neighborhood of the optimal steady-state for the closed-loop system resulting from the application of economic model predictive control schemes. The validity of the results is shown in a simulation environment considering the problem of the optimal power split in hybrid electric vehicles.

Keywords: dissipativity, economic model predictive control, hybrid electric vehicles

1. INTRODUCTION

Dissipativity is a well-known and essential concept of system and control theory introduced by Willems (1972a,b). Against this background, renewed interest on this property has been shown in the context of Economic Model Predictive Control (EMPC). EMPC is a particular kind of Model Predictive Control (MPC) characterized by general objective functions (Faulwasser et al. (2018)). Analogously to MPC, at each time step the control inputs are computed solving a finite horizon optimal control problem. Then, only the first component of the predicted input sequence is applied to the system. In this scenario, dissipativity properties are extremely useful in order to characterize the optimal operating behavior of a system and to analyze closed-loop convergence, see Faulwasser et al. (2018) and Müller et al. (2015). Results available in the literature prove dissipativity conditions for dynamical systems modeled by difference equations (see, *e.g.*, Damm et al. (2014) and Berberich et al. (2020)). In particular, strict dissipativity is employed to characterize optimal steady-state (Faulwasser et al. (2018); Müller et al. (2015)) and optimal periodic operation (Zanon et al. (2017); Köhler et al. (2018)). Once dissipativity conditions are provided, these can be used to guarantee convergence of the closed-loop system, obtained from the application of EMPC schemes, to the optimal behavior (Faulwasser et al. (2018)).

This work proposes some preliminary results on dissipativity conditions for systems modeled by convex difference inclusions. These findings are extremely important in order to retrieve convergence guarantees for generic EMPC schemes built on such systems. This turns out to be fundamental for the development of effective online energy management strategies for hybrid electric vehicles. In this paper, some available results on optimal operation at steady-state proposed by Damm et al. (2014) are extended to the case of dynamical systems described by convex difference inclusions. Thus, the main contributions are summarized as follows:

- Considering a system described by convex difference inclusions, dissipativity is proven for optimal steady-state operation. This property provides important information on the convergence of the closed-loop system obtained by applying EMPC schemes.
- Implications of the dissipativity result for the energy management strategy problem of hybrid electric vehicles are discussed.

The paper is organized as follows. First, dissipativity is proven for steady-state operation of dynamical systems modeled by convex difference inclusions (Section 2). Then, in Section 3, the validity of the dissipativity condition and of its implications is shown, in a simulation environment, for the energy management problem of hybrid electric vehicles.

2. DISSIPATIVITY CONDITION FOR OPTIMAL STEADY-STATE OPERATION

In this section, the strict dissipativity condition for optimal operation at steady-state is proven. First, the general convex program is formulated. Then, dissipativity is analyzed. Eventually, an EMPC formulation is provided.

2.1 Problem formulation

The system dynamics is modeled by the following difference inclusion:

$$\begin{aligned} x(k+1) \in F(x(k), u(k), r(k)) = \\ = \{y \in \mathbb{R}^n | y \leq f(x(k), u(k), r(k))\}, \end{aligned} \tag{1}$$

where f is a concave and continuous function. Moreover, $x \in \mathbb{R}^n$ denotes the state variables, $u \in \mathbb{R}^m$ the control variables, and $r \in \mathbb{R}^w$ some reference signals. Therefore, the feasible tuples (x, u, r) are collected in the following set, which is assumed to be compact:

$$\mathbb{Y} := \{(x, u, r) \in \mathbb{R}^n \times \mathbb{R}^m \times \mathbb{R}^w | g_i(x, u, r) \leq 0 \text{ for all } g_i \in \mathcal{G}\} \tag{2}$$

with $\mathcal{G}$ the set of constraints and $g_i : \mathbb{R}^n \times \mathbb{R}^m \times \mathbb{R}^w \to \mathbb{R}$ convex. Hence, the following sets are defined:

$$\mathbb{X} := \{x \in \mathbb{R}^n | \exists\ u \in \mathbb{R}^m \text{ and } r \in \mathbb{R}^w \text{ with } (x, u, r) \in \mathbb{Y}\},$$
$$\mathbb{U} := \{u \in \mathbb{R}^m | \exists\ x \in \mathbb{R}^n \text{ and } r \in \mathbb{R}^w \text{ with } (x, u, r) \in \mathbb{Y}\}.$$

Eventually, the general convex optimal control problem (defined over the horizon $\mathcal{N}$) reads as follows:

$$\begin{aligned} \underset{x(0),u(0),\ldots,x(\mathcal{N})}{\text{minimize}} \quad & \sum_{k=0}^{\mathcal{N}-1} l(x(k), u(k), r(k)) + V_f(x(\mathcal{N})) \\ \text{subject to} \quad & x(k+1) \in F(x(k), u(k), r(k)) = \\ & = \{y \in \mathbb{R}^n | y \leq f(x(k), u(k), r(k))\} \\ & g_i(x(k), u(k), r(k)) \leq 0,\ \forall g_i \in \mathcal{G} \end{aligned} \tag{3}$$

with l being the continuous and convex stage cost and V_f a suitable continuous and convex terminal cost. In the EMPC context, program (3) is solved with $x(0) = x(t)$ (the measured state) over a suitable prediction horizon $\mathcal{N} = N_p$. Then, only the first control variable is applied to the system (receding horizon principle).

2.2 Optimal steady-state operation

Let us introduce $(x^\star, u^\star, \bar{r})$, the optimal steady-state (or equilibrium point) retrieved from the solution of the following convex program:

$$\begin{aligned} \underset{x,u}{\text{minimize}} \quad & l(x, u, \bar{r}) \\ \text{subject to} \quad & x \leq f(x, u, \bar{r}) \\ & g_i(x, u, \bar{r}) \leq 0,\ \forall g_i \in \mathcal{G} \end{aligned} \tag{4}$$

where $\bar{r}$ is a constant reference signal and g_i and $x - f(x, u, \bar{r})$ are convex in $(x, u, \bar{r})$. The equilibrium tuple $(x^\star, u^\star, \bar{r})$, solution of (4), satisfies $l(x^\star, u^\star, \bar{r}) \leq l(\tilde{x}^\star, \tilde{u}^\star, \bar{r})$ for all other equilibrium tuples $(\tilde{x}^\star, \tilde{u}^\star, \bar{r}) \in \mathbb{Y}$.

Definition 2.1. *Let $(x^\star, u^\star, \bar{r}) \in \mathbb{Y}$ be an equilibrium point of (1), with $\bar{r}$ a constant reference signal. The system (1) is dissipative with respect to the supply rate $s(x, u, \bar{r}) = l(x, u, \bar{r}) - l(x^\star, u^\star, \bar{r})$ if there exists a storage function $\lambda : \mathbb{X} \to \mathbb{R}$ bounded from below such that the inequality:*

$$\lambda(x^+) - \lambda(x) \leq s(x, u, \bar{r}) \tag{5}$$

holds for all $(x, u, \bar{r}) \in \mathbb{Y}$ and all $x^+ \in F(x, u, \bar{r})$ (with x^+ denoting the time difference). The system is strictly dissipative if there exists $\alpha \in \mathcal{K}_\infty$ [1] such that the following holds for all $(x, u, \bar{r}) \in \mathbb{Y}$ and all $x^+ \in F(x, u, \bar{r})$:

$$\lambda(x^+) - \lambda(x) + \alpha(\| (x - x^\star, u - u^\star) \|) \leq s(x, u, \bar{r}). \tag{6}$$

[1] $\mathcal{K}_\infty := \{\alpha \in \mathcal{K} | \alpha \text{ is unbounded}\}$ and
$\mathcal{K} := \{\alpha : \mathbb{R}_+ \to \mathbb{R}_+ | \alpha \text{ continuous, strictly increasing, } \alpha(0) = 0\}$.

The validity of dissipativity as per Definition 2.1 implies optimal steady-state operation. This means that, on average, no other solution can outperform the optimal steady-state. Furthermore, this property allows to conclude closed-loop convergence to a neighborhood of the the optimal steady-state when controlling the system with the EMPC scheme (3), compare Faulwasser et al. (2018). Against this background, it can be shown that this dissipativity property holds for convex difference inclusions subject to strictly convex cost and convex constraints, as will be done in the following.

Proposition 2.1. *Consider the optimal control problem (3) with dynamics (1), strictly convex l, a constraint set defined as in (2) with g_i convex, and a constant reference signal $\bar{r}$. Assume (4) to satisfy Slater's condition, i.e., there exists $(\hat{x}, \hat{u}, \bar{r}) \in \mathbb{Y}$ such that:*

$$\begin{aligned} \hat{x} - f(\hat{x}, \hat{u}, \bar{r}) < 0, \\ g_i(\hat{x}, \hat{u}, \bar{r}) < 0,\ \forall g_i \in \mathcal{G}. \end{aligned} \tag{7}$$

Then, there exists a vector $\nu_f \in \mathbb{R}^n_+$ such that the system is strictly dissipative with respect to the supply rate $s(x, u, \bar{r}) = l(x, u, \bar{r}) - l(x^\star, u^\star, \bar{r})$ and with $\lambda(x) = \nu_f^T x$.

The proof is an extension of the work proposed by Damm et al. (2014) to convex difference inclusions.

Proof. The strict convexity of l, together with the convexity and compactness of the constraints, ensures that the optimization problem (4) has a global and unique optimum $(x^\star, u^\star, \bar{r})$. Therefore, the Lagrangian for program (4) is introduced:

$$\mathcal{L}(x, u, \bar{r}) := l(x, u, \bar{r}) + (\nu_g^T, \nu_f^T) \begin{pmatrix} g_1(x, u, \bar{r}) \\ \vdots \\ g_i(x, u, \bar{r}) \\ x - f(x, u, \bar{r}) \end{pmatrix}. \tag{8}$$

The validity of the Slater's condition implies strong duality (Boyd and Vandenberghe (2004)), *i.e.*, the existence of Lagrange multipliers ν_g and ν_f such that:

$$\begin{aligned} \nu_g \geq 0,\ \nu_f \geq 0 \text{ and} \\ \nu_g = 0,\ \text{if } g_i(x^\star, u^\star, \bar{r}) < 0 \\ \nu_f = 0,\ \text{if } x^\star - f(x^\star, u^\star, \bar{r}) < 0, \end{aligned} \tag{9}$$

and such that the following inequality holds:

$$\mathcal{L}^\star(x^\star, u^\star, \bar{r}) < \mathcal{L}(x, u, \bar{r}), \quad \forall\ (x, u, \bar{r}) \neq (x^\star, u^\star, \bar{r}). \tag{10}$$

Let us define $\widehat{L}$ as follows:

$$\widehat{L}(x, u, \bar{r}) := l(x, u, \bar{r}) - l(x^\star, u^\star, \bar{r}) + (\nu_g^T, \nu_f^T) \begin{pmatrix} g_1(x, u, \bar{r}) \\ \vdots \\ g_i(x, u, \bar{r}) \\ x - f(x, u, \bar{r}) \end{pmatrix}. \tag{11}$$

Therefore, from (10) and (11):

$$\widehat{L}(x, u, \bar{r}) > (\nu_g^T, \nu_f^T) \begin{pmatrix} g_1(x^\star, u^\star, \bar{r}) \\ \vdots \\ g_i(x^\star, u^\star, \bar{r}) \\ x^\star - f(x^\star, u^\star, \bar{r}) \end{pmatrix} = 0 \tag{12}$$

for all $(x, u, \bar{r}) \neq (x^\star, u^\star, \bar{r})$, due to the complementary slackness condition (9). Given that $\nu_g^T[g_1(x, u, \bar{r}) \ldots g_i(x, u, \bar{r})]^T \leq 0$ for all $(x, u, \bar{r}) \in \mathbb{Y}$, $\widehat{L}$ is bounded from above on $\mathbb{Y}$ as follows:

$$L(x, u, \bar{r}) := l(x, u, \bar{r}) - l(x^\star, u^\star, \bar{r}) + \nu_f^T(x - f(x, u, \bar{r})) \geq \widehat{L}(x, u, \bar{r}). \tag{13}$$

Now consider any tuple $(x, u, \bar{r}) \in \mathbb{Y}$ together with x^+ satisfying the difference inclusion (1), *i.e.*,

$$x^+ \leq f(x, u, \bar{r}). \tag{14}$$

Since $\nu_f \geq 0$, for any such points the following inequality must hold:

$$\begin{aligned} L'(x, u, \bar{r}, x^+) &:= l(x, u, \bar{r}) - l(x^\star, u^\star, \bar{r}) + \nu_f^T(x - x^+) \geq \\ &\geq L(x, u, \bar{r}) \geq \widehat{L}(x, u, \bar{r}). \end{aligned} \tag{15}$$

That is, if (14) holds with strict inequality, $\widehat{L}$ is strictly bounded from above by L'. Choosing the storage function $\lambda(x) = \nu_f^T x$, from (15) the desired strict dissipativity result follows if there exists some $\alpha \in \mathcal{K}_\infty$, such that the following inequality holds for all $(x, u, \bar{r}) \in \mathbb{Y}$ and for all x^+ satisfying (14):

$$L'(x, u, \bar{r}, x^+) \geq \alpha(\| (x - x^\star, u - u^\star) \|). \tag{16}$$

Since $L'(x, u, \bar{r}, x^+) > 0$ for all $(x, u, \bar{r}) \in \mathbb{Y}$ and x^+ satisfying (14) with $(x, u, \bar{r}, x^+) \neq (x^\star, u^\star, \bar{r}, x^\star)$ and $L'(x^\star, u^\star, \bar{r}, x^\star) = 0$, Lemma A.1 of Berberich et al. (2020) can be applied to prove the validity of (16), thus ensuring strict dissipativity. □

3. SIMULATION RESULTS FOR THE ENERGY MANAGEMENT PROBLEM OF HEVS

The implications of the dissipativity condition proved in Section 2 are discussed. In particular, the problem of the energy management strategy of hybrid electric vehicles is addressed. The presence of multiple power sources (the Li-ion battery and the internal combustion engine) offers a power split feature, which must be carefully controlled to achieve the best possible energy efficiency. In this work, an Extended Range Electric Vehicle (EREV) is considered. This particular kind of hybrid electric vehicles is the composition of an electric vehicle and of a Range EXtender (REX). Thus, a powertrain modeling is introduced. Then, the energy management problem is formalized as an optimal control problem and convergence of the MPC solution to a neighborhood of the optimal steady-state is shown.

3.1 Modeling

The energy management strategy problem is formalized as a mixed-integer convex program (Section 3.2). Therefore, a convex powertrain modeling is recalled. In particular, a backward modeling paradigm, as per Onori et al. (2016), is employed and the power needed for the vehicle motion is computed from driving cycle speed (v) and slope (θ) profiles. The propulsion system components are highlighted in Figure 1. To ease readers' comprehension, the model is proposed in continuous time. Eventually, the principal powertrain parameters are summarized in Table 1. For further details on the propulsion system modeling, readers' are referred to Pozzato et al. (2019, 2020).

Vehicle dynamics. The vehicle motion is described by the following longitudinal dynamics equation:

$$T_w = R_w(M\dot{v} + F_b + F_f), \quad \omega_w = \frac{v}{R_w} \tag{17}$$

with M the vehicle mass, T_w the wheel torque, ω_w the wheel rotational speed, and R_w the wheel radius. F_b is the mechanical braking force and F_f is the friction force accounting for both drag and rolling resistance.

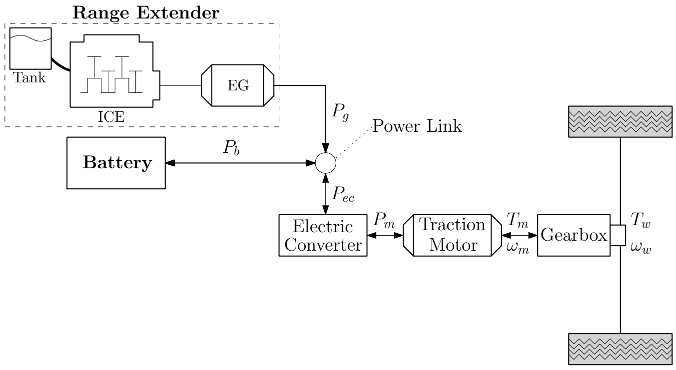

Fig. 1: EREV powertrain (ICE: Internal Combustion Engine, EG: Electric Generator).

Gearbox. A constant ratio transmission r_t connects the wheels to the traction motor:

$$T_m = \begin{cases} \frac{1}{r_t \eta_t} T_w, & \text{if } T_w \geq 0 \text{ (traction)} \\ \frac{\eta_t}{r_t} T_w, & \text{if } T_w < 0 \text{ (braking)} \end{cases}, \quad \omega_m = r_t \omega_w \tag{18}$$

with ω_m the motor rotational speed, T_m the motor torque, and η_t the transmission efficiency.

Traction motor. The traction motor is modeled as an efficiency map η_m. Therefore, the electric power P_m in motor and generator modes is modeled as follows:

$$P_m = \begin{cases} \frac{T_{m,i}\omega_m}{\eta_m(T_{m,i}, \omega_m)}, & \text{if } T_{m,i} \geq 0 \text{ (motor)} \\ T_{m,i}\omega_m \eta_m(T_{m,i}, \omega_m), & \text{if } T_{m,i} < 0 \text{ (generator)} \end{cases} \tag{19}$$

where J_m is the motor inertia and $T_{m,i} = T_m + J_m \dot{\omega}_m$.

Electric converter. The electric converter is modeled as an average efficiency η_{ec} (Hu et al. (2013)):

$$P_{ec} = \begin{cases} \frac{P_m}{\eta_{ec}}, & \text{if } P_m \geq 0 \\ P_m \eta_{ec}, & \text{if } P_m < 0 \end{cases} \tag{20}$$

with P_{ec} the power requested by the driving cycle.

Power link. Given the presence of multiple power sources, the power requested by the drivetrain must satisfy the following balance equation:

$$P_{ec} = P_b + P_g \tag{21}$$

P_b is the absorbed/supplied battery power and P_g is the REX generated power.

Battery model. The battery is modeled in terms of its internal energy E (Elbert et al. (2014)):

$$\begin{aligned} \dot{E} = \phi(E, P_b, P_{ec}) &= -\frac{A_b}{R_b Q_b}(E + E_0) \\ &+ \frac{A_b}{R_b Q_b}\sqrt{(E + E_0)^2 - \frac{2R_b Q_b}{A_b} P_b (E + E_0)} \end{aligned} \tag{22}$$

with $E_0 = \frac{Q_b}{2A_b} B_b^2$ and P_b obtained from (21). Equation (22) is non-convex but the term on the right hand side of (22) is concave. Therefore, the battery model is relaxed introducing the following differential inclusion:

$$\dot{E} \in \Phi(E, P_b, P_{ec}) = \{y \in \mathbb{R} | y \leq \phi(E, P_b, P_{ec})\} \tag{23}$$

with Φ the *hypograph* of ϕ: a convex set given the concavity of ϕ. According to Elbert et al. (2014) and assuming the presence of a cost function accounting for the battery usage, the relaxation (23) does not affect the accuracy of the solution. Eventually, the following inequality must always be satisfied $P_b \leq (E + E_0)\frac{A_b}{2Q_b R_b}$.

Range extender. The REX is a device composed of a diesel internal combustion engine coupled with an electric generator. Therefore, the mechanical power generated by the internal combustion engine is converted into electrical power and used to provide energy to the electric drivetrain.

Power generation. The electric generated power takes values in the following range: $2 \leq P_g \leq 35 \ \cup \ 0$ (kW). If the REX is idling, P_g is equal to 0 (kW). The fuel thermal power is approximated by a second order polynomial function (Murgovski et al. (2012)):

$$P_f = A_g P_g^2 + B_g P_g + C_g \tag{24}$$

where A_g, B_g, and C_g are identified parameters. The REX provides power to the traction motor only if the power request exceeds P_{thr}. This behavior is modeled as follows:

$$q(P_{ec}) = \begin{cases} 1, & P_{ec} > P_{thr} \\ 0, & \text{otherwise.} \end{cases} \tag{25}$$

The maximum power $\overline{P_g}(\overline{T}) = 35$ (kW) is provided if the REX is warmed-up. Thus, once the vehicle is turned on, for the first 6 (min) (the time needed to warm-up the engine) the maximum power is limited to $\overline{P_g}(\underline{T}) = 27$ (kW). Eventually, the REX operating conditions are summarized as follows:

$$\begin{cases} q(P_{ec})\underline{P_g} \leq P_g \leq q(P_{ec})\overline{P_g}(\underline{T}), & \text{warm-up phase} \\ q(P_{ec})\underline{P_g} \leq P_g \leq q(P_{ec})\overline{P_g}(\overline{T}), & \text{warmed-up engine} \end{cases} \tag{26}$$

with $\underline{P_g}$ the minimum electric power which can be generated by the REX.

Noise modeling. According to Pozzato et al. (2019), the following relationship is introduced to model noise emissions:

$$L_p = A_{SPL} P_g + B_{SPL} \tag{27}$$

with A_{SPL} and B_{SPL} identified parameters. Noise emissions are characterized by Sound Pressure Levels (SPL) and expressed in dB(A) (Cory (2010)).

3.2 Energy management problem

The energy management strategy has the primal goal of splitting the power request between the available movers. To this aim, the battery model (23) is first discretized. Then, the energy management problem is formalized as a mixed-integer convex program over a finite time horizon N.

Discretized Battery Model. (23) is discretized as follows:

$$E(k+1) = E(k) - T_s \frac{A_b}{Q_b R_b}(E(k) + E_0) + T_s \frac{A_b}{Q_b R_b}\sqrt{(E(k) + E_0)^2 - \frac{2R_b Q_b}{A_b} P_b(k)(E(k) + E_0)} \tag{28}$$

where T_s is the sampling time. Far from the SoC upper and lower bounds, (28) is well approximated by the battery energy difference ΔE:

Variable	Description	Unit	Value
Vehicle			
M	Vehicle mass (with battery pack)	(kg)	12635
R_w	Wheel radius (Hu et al. (2013))	(m)	0.509
η_t	Transmission efficiency (Hu et al. (2013))	$(-)$	0.97
r_t	Gear ratio (Hu et al. (2013))	$(-)$	4.7
J_m	Electric motor inertia (Hu et al. (2015))	(kg m^2)	2.3
η_{ec}	Electric converter efficiency (Hu et al. (2013))	$(-)$	0.98
Battery			
A_b	Voltage parameter	(V)	27.10
B_b	Voltage parameter	(V)	585.951
V_b	Nominal voltage	(V)	600
Q_b	Nominal capacity	(Ah)	107
N_b	Nominal life cycle	$(-)$	4000
σ_b	Severity factor (20 − 35 (°C)) (Suri and Onori (2016))	$(-)$	0.95
η_{grid}	Charging efficiency (Xiong et al. (2009))	$(-)$	0.92
$\overline{P_b}$	Maximum power (Hu et al. (2013))	(kW)	220
$\underline{P_b}$	Minimum power (Hu et al. (2013))	(kW)	−220
$\overline{SoC}$	Maximum SoC	(%)	80
$\underline{SoC}$	Minimum SoC	(%)	20
$\overline{\Delta E}$	Maximum ΔE	(kJ)	216.8
$\underline{\Delta E}$	Minimum ΔE	(kJ)	223.6
REX			
A_{SPL}	Noise parameter	(dB(A)/kW)	Confidential
B_{SPL}	Noise parameter	(dB(A))	Confidential
A_g	Generated power parameter	(1/kW)	Confidential
B_g	Generated power parameter	$(-)$	Confidential
C_g	Generated power parameter	(kW)	Confidential
$p_g^{(1)}$	Generated power breakpoint	(kW)	20
$p_g^{(2)}$	Generated power breakpoint	(kW)	25
$\overline{T}$	Coolant warmed-up temperature	(°C)	60
$\underline{T}$	Room temperature	(°C)	20
P_{thr}	Idling power threshold	(kW)	2
$\overline{P_g}(\overline{T})$	Maximum power (warmed-up)	(kW)	35
$\overline{P_g}(\underline{T})$	Maximum power (cold)	(kW)	27
$\underline{P_g}$	Minimum power	(kW)	2
Cost Function			
T_s	Sampling time	(s)	1
$\alpha_€$	Grid energy cost	(€ kW^{-1} h^{-1})	0.125
$\beta_€$	Battery cost	(€ kW^{-1} h^{-1})	400
$\gamma_€$	REX fuel cost	(€ kW^{-1} h^{-1})	0.104
$\delta_{€,0}$	REX noise cost (baseline)	(€ dB(A)$^{-1}$ h^{-1})	0.018

Table 1: Application parameters.

$$\Delta E(k+1) = f(\Delta E(k), P_b(k), P_{ec}(k)) = -T_s \frac{A_b}{R_b Q_b}(\Delta E(k) + E_0) + T_s \frac{A_b}{R_b Q_b}\sqrt{(\Delta E(k) + E_0)^2 - \frac{2R_b Q_b}{A_b} P_b(k)(\Delta E(k) + E_0)}. \tag{29}$$

Thus, at each time instant k, the battery energy is computed with the following cumulative sum:

$$E(k) = E(0) + \sum_{i=0}^{k} \Delta E(i) \tag{30}$$

with $E(0)$ the battery internal energy initial condition. The right hand side of (29) is concave, therefore, the convex model is obtained introducing the *hypograph* reformulation (in accordance with (23)):

$$\begin{aligned}\Delta E(k+1) \in F(\Delta E, P_b, P_{ec}) = \\ = \{y \in \mathbb{R} | y \leq f(\Delta E(k), P_b(k), P_{ec}(k))\}.\end{aligned} \tag{31}$$

(29) fits well with the EMS formulation, detailed in what follows. Indeed, the battery utilization is a function of ΔE and not of E. This is appropriate because, far away from the state of charge bounds, the battery power is bounded between $\left[\underline{P_b}, \overline{P_b}\right]$, independent of the actual SoC value.

Mixed-integer convex program. Given the control variables P_g and P_b, the exogenous inputs P_{ec} and $q(P_{ec})$, and the state variable ΔE, the mixed-integer convex program reads as follows:

$$\begin{aligned}
\underset{\Delta E, P_g, P_b}{\text{minimize}} \quad & \left.-\tfrac{\alpha_{€}}{\eta_{grid}}\Delta E(N) + \right\} V_f \\
& \left. T_s \sum_{k=0}^{N-1} \tfrac{\alpha_{€}}{\eta_{grid}} \tfrac{-\Delta E(k)}{T_s} + \right\} l_1 \\
& \left.\begin{aligned}
& T_s \sum_{k=0}^{N-1} \beta_{€} \tfrac{\sigma_b}{N_b} \mid P_b(k) \mid \; + \\
& T_s \sum_{k=0}^{N-1} \gamma_{€} (A_g P_g(k)^2 + B_g P_g(k) + C_g) + \\
& T_s \sum_{k=0}^{N-1} \delta_{€,0} \mathrm{SF}(v) \Big[(A_{SPL} P_g^{(1)}(k) + B_{SPL}) + \\
& \qquad (2A_{SPL} P_g^{(2)}(k) + q_{SPL}^{(1)}(k) B_{SPL}) + \\
& \qquad (A_{SPL} P_g^{(3)}(k) - q_{SPL}^{(2)}(k) B_{SPL}) \Big] +
\end{aligned}\right\} l_2
\end{aligned} \tag{32}$$

subject to

$$\begin{aligned}
& \Delta E(k+1) \in F(\Delta E, P_b, P_{ec}) = \\
& \qquad = \{y \in \mathbb{R} | y \leq f(\Delta E(k), P_b(k), P_{ec}(k))\} \\
& P_{ec}(k) \leq P_b(k) + P_g(k) \\
& \underline{\Delta E} \leq \Delta E(k) \leq \overline{\Delta E} \\
& \underline{P_b} \leq P_b(k) \leq \overline{P_b} \\
& P_b(k) \leq (\Delta E(k) + E_0) \frac{A_b}{2 Q_b R_b} \\
& \begin{cases} q(P_{ec}) \underline{P_g} \leq P_g(k) \leq q(P_{ec}) \overline{P_g}(\underline{T}), & \text{warm-up phase} \\ q(P_{ec}) \underline{P_g} \leq P_g(k) \leq q(P_{ec}) \overline{P_g}(\overline{T}), & \text{warmed-up engine} \end{cases} \\
& p_g^{(1)} q_{SPL}^{(1)}(k) \leq P_g^{(1)}(k) \leq p_g^{(1)} \\
& (p_g^{(2)} - p_g^{(1)}) q_{SPL}^{(2)}(k) \leq P_g^{(2)}(k) \leq q_{SPL}^{(1)}(k)(p_g^{(2)} - p_g^{(1)}) \\
& 0 \leq P_g^{(3)}(k) \leq q_{SPL}^{(2)}(k)(\overline{P_g}(\overline{T}) - p_g^{(2)})
\end{aligned} \tag{33}$$

Eventually, the following initial condition is introduced:

$$\Delta E(0) = 0 \text{ (kJ)}.$$

The cost function is composed of four terms. V_f and l_1 model the electrical energy needed to replace the battery energy depleted during the driving cycle. Considering l_2, the first term from above is accounting for battery aging. Thus, the second one is considering the fuel consumption and the third one is weighting the REX noise emissions. For the problem at hand, P_g takes the following expression: $P_g(k) = P_g^{(1)}(k) + P_g^{(2)}(k) + P_g^{(3)}(k)$. However, to simplify the notation, in (32) and (33), P_g is used when possible. Further details on the cost function formulation can be found in Pozzato et al. (2019, 2020).

	Offline	**MPC**		
N_p (s)	NA	2	50	100
SoC (%)	45.8269	45.9113	45.8192	45.8226
J (€)	1.7589	1.7600	1.7599	1.7599
J_e (€)	0.3634	0.3560	0.3640	0.3637
J_a (€)	0.2539	0.2488	0.2544	0.2542
J_f (€)	0.5337	0.5464	0.5331	0.5336
J_n (€)	0.6079	0.6087	0.6084	0.6084
Opt. time	71.6 (s)	0.008 (s/step)	0.036 (s/step)	0.098 (s/step)

* NA: Not Applicable

Table 2: Sensitivity analysis with respect to different prediction horizons N_p. The EMPC results are compared to the optimal steady-state solution applied over a traveled distance of 10 (km).

3.3 Results

The validity of the dissipativity condition, proved in Section 2, is shown for the problem at hand. First, the following definitions (needed to make a direct correspondence with Section 2) are introduced:

- $x := \Delta E$ is the state variable;
- $u := [P_g^{(1)} \; P_g^{(2)} \; P_g^{(3)} \; P_b]^T$ are the control inputs;
- $r := P_{ec}$ is the reference signal.

Against this background, the stage cost $l : \mathbb{Y} \to \mathbb{R}$ takes the following structure:

$$\begin{aligned} l(x(k), u(k), r(k)) = l_1(x(k)) + l_2(u(k), r(k)) = \\ = -\xi x(k) + l_2(u(k), r(k)) \end{aligned} \tag{34}$$

where l_1 and l_2 are defined as in (32) and $\xi = \frac{\alpha_{€}}{\eta_{grid}} \in \mathbb{R}_+ \backslash \{0\}$. The MPC is formalized according to (3), starting from (32),(33). In this framework, the limitation (26) on the REX generated power is formulated relying on two complementary formulations of (3). Therefore, for the first 6 (min) of operation the MPC embeds the constraint with $\overline{P_g}(\underline{T})$. Conversely, once the engine is warmed-up, the constraint with $\overline{P_g}(\overline{T})$ is employed.

The REX is now assumed to be warmed-up and a constant speed profile at 30 (km/h), along with a constant power request of $\bar{r} = 11.23$ (kW) (the vehicle is assumed to be already at the target speed and the acceleration transient is neglected), is considered. Therefore, the optimal steady-state is computed solving (4), which leads to:

$$P_b^\star = 8.03 \text{ (kW)}, \; P_g^\star = 3.20 \text{ (kW)}, \; \Delta E^\star = -8.03 \text{ (kJ)}. \tag{35}$$

The system (31) is proven to be dissipative with respect to (35) checking the validity of (5) for all $(x, u, \bar{r}) \in \mathbb{Y}$. Thus, (5) is rewritten as follows:

$$\nu_f (f(x, u, \bar{r}) - x) \leq l(x, u, \bar{r}) - l(x^\star, u^\star, \bar{r}). \tag{36}$$

For $\nu_f = 0.038$ (€/MJ) (retrieved from the solution of the dual problem of (4)), the previous inequality holds true. This implies that, for a long enough prediction horizon, the solution of the EMPC without terminal constraints defined in (3) converges to a neighborhood of the optimal steady-state (35). This fact is shown solving the

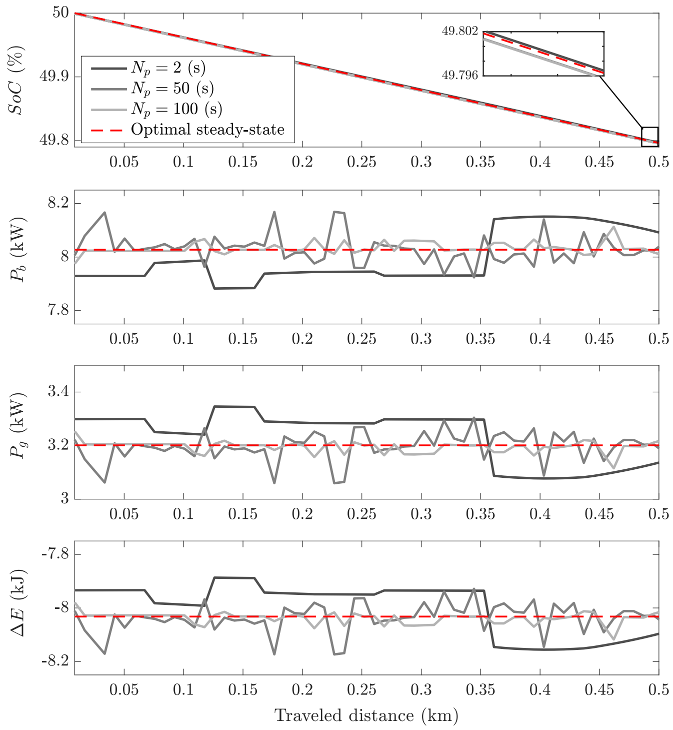

Fig. 2: Solution of (3) *considering different values of the prediction horizon* N_p*. Increasing* N_p*, the MPC solution approaches the optimal steady-state. Solutions are zoomed between* 0 *and* 500 (*m*)*.*

EMPC problem assuming the vehicle is traveling over a distance of 10 (km) while maintaining a constant speed of 30 (km/h). As shown by Figure 2, increasing N_p the MPC approaches the optimal steady-state at the cost of an increased optimization time (see Table 2). The MPC prediction is performed assuming a perfect knowledge of the future driving cycle.

4. CONCLUSIONS

In this work, a strict dissipativity result for the optimal steady-state operation of systems modeled by convex difference inclusions is shown. This property allows to retrieve convergence guarantees for the closed-loop system obtained applying EMPC schemes. To illustrate this fact, a simulation study is performed considering the power split issue for EREV.

Future work will provide insights on strict dissipativity conditions for the optimal periodic operation of systems described by convex difference inclusions. Thorough simulation studies will be performed to prove the validity and the implications of such strict dissipativity properties in the particular context of hybrid electric vehicles.

ACKNOWLEDGEMENT

This work was partially sponsored by Steyr Motors GmbH and the Linz Center of Mechatronics (LCM).

REFERENCES

Berberich, J., Köhler, J., Allgöwer, F., and Müller, M.A. (2020). Dissipativity properties in constrained optimal control: a computational approach. *Automatica*, 114, 108840.

Boyd, S. and Vandenberghe, L. (2004). *Convex optimization*. Cambridge university press.

Cory, W. (2010). Relationship between sound pressure and sound power levels. *2010 Eurovent. WG*, 1.

Damm, T., Grüne, L., Stieler, M., and Worthmann, K. (2014). An exponential turnpike theorem for dissipative discrete time optimal control problems. *SIAM Journal on Control and Optimization*, 52(3), 1935–1957.

Elbert, P., Nüesch, T., Ritter, A., Murgovski, N., and Guzzella, L. (2014). Engine on/off control for the energy management of a serial hybrid electric bus via convex optimization. *IEEE Transactions on Vehicular Technology*, 63(8), 3549–3559.

Faulwasser, T., Grüne, L., Müller, M.A., et al. (2018). Economic nonlinear model predictive control. *Foundations and Trends® in Systems and Control*, 5(1), 1–98.

Hu, X., Murgovski, N., Johannesson, L., and Egardt, B. (2013). Energy efficiency analysis of a series plug-in hybrid electric bus with different energy management strategies and battery sizes. *Applied Energy*, 111, 1001–1009.

Hu, X., Murgovski, N., Johannesson, L.M., and Egardt, B. (2015). Optimal dimensioning and power management of a fuel cell/battery hybrid bus via convex programming. *IEEE/ASME transactions on mechatronics*, 20(1), 457–468.

Köhler, J., Müller, M.A., and Allgöwer, F. (2018). On periodic dissipativity notions in economic model predictive control. *IEEE Control Systems Letters*, 2(3), 501–506.

Müller, M.A., Grüne, L., and Allgöwer, F. (2015). On the role of dissipativity in economic model predictive control. *IFAC-PapersOnLine*, 48(23), 110–116.

Murgovski, N., Johannesson, L., Sjöberg, J., and Egardt, B. (2012). Component sizing of a plug-in hybrid electric powertrain via convex optimization. *Mechatronics*, 22(1), 106–120.

Onori, S., Serrao, L., and Rizzoni, G. (2016). *Hybrid electric vehicles: Energy management strategies*. Springer.

Pozzato, G., Formentin, S., Panzani, G., and Savaresi, S.M. (2019). Least costly energy management for extended-range electric vehicles with noise emissions characterization. In 9^{th} *International Symposium on Advances in Automotive Control*. IFAC.

Pozzato, G., Formentin, S., Panzani, G., and Savaresi, S.M. (2020). Least costly energy management for extended-range electric vehicles: an economic optimization framework. *European Journal of Control*.

Suri, G. and Onori, S. (2016). A control-oriented cycle-life model for hybrid electric vehicle lithium-ion batteries. *Energy*, 96, 644–653.

Willems, J.C. (1972a). Dissipative dynamical systems part i: General theory. *Archive for rational mechanics and analysis*, 45(5), 321–351.

Willems, J.C. (1972b). Dissipative dynamical systems part ii: Linear systems with quadratic supply rates. *Archive for rational mechanics and analysis*, 45(5), 352–393.

Xiong, W., Zhang, Y., and Yin, C. (2009). Optimal energy management for a series–parallel hybrid electric bus. *Energy conversion and management*, 50(7), 1730–1738.

Zanon, M., Grüne, L., and Diehl, M. (2017). Periodic optimal control, dissipativity and mpc. *IEEE Transactions on Automatic Control*, 62(6), 2943–2949.